VOL. 22, NO. 3, 2023, 37-45
elektrika.utm.my
ISSN 0128-4428

ELEKTRIKA
Journal of Electrical Engineering

Comparison of APF and STATCOM for Current Harmonic Mitigation

Abdul Rahman Galadima and **Rasyidah Binti Mohamad Idris***

Faculty of Electrical Engineering, Universiti Teknologi Malaysia, 81310 UTM Skudai, Johor, Malaysia.

*Corresponding author: rasyidahidris@utm.my

Abstract: The application of solid-state electronic devices has recorded a geometric increase in the last decade. Devices such as battery charging systems, inverters, switch mode power supplies and a host of electronic-based devices referred to as non-linear loads distort the source signal (particularly the current). Harmonics distortion imposes a severe impact on the well-being of the power system. They cause excessive device heating, reduced performance efficiency, early insulation failure, decreased dynamic torque in rotating systems, etc. This paper bases a study on Active Power Filter (APF) and Static Synchronous Compensator (STATCOM) for mitigation of these distortive harmonics in a system of 3-phase 11kV/400V, 400kVA feeding a system of non-linear loads. The study is based on the IEEE519 standard limits for current harmonics measured at the PCC. Therefore, the system short circuit ratio (SCR) is first determined. Using synchronous reference frame and instantaneous reactive power theories, the APF and STATCOM are respectively designed and run using MATLAB/Simulink software. The result analysis is obtained from the FFT signal processing toolbox of the software, and the device's performances are evaluated based on the set standard. Results from the FFT spectra showed that the model system contains a considerable number of harmonics before filtering. However, when these devices are connected to the system, all higher-order harmonics have been minimized to the least fractions with respect to the standard, with STATCOM giving a comparatively better performance.

Keywords: STATCOM, APF, harmonic mitigation, nonlinear load, FFT analysis

Article History: received 1 March 2023; accepted 25 October 2023; published 26 December 2023.

1. INTRODUCTION

The current global increase in the use of solid-state devices does not need technical explanation [1]. In both commercial and residential buildings, the use of Computer systems, adjustable speed drives (ASD), fluorescent lamps, inverter-based air-conditioners, light-emitting diode (LED) lamps, battery charging systems, etc. have recorded a tremendous growth in the last decades [2], [3]. In advance technologies, electric vehicles (EVs) with their charging stations is emerging development [4]. These power electronics generally referred to as non-linear loads, employ various power conversion topologies for their operations [5], [6]. This leads to imposition of severe harmonics in the power systems.

Harmonics is one of the major obstacles to a stable, reliable, and sustainable power supply [6]. Some of the noticeable and severe consequences of harmonics in power systems include core, hysteresis and eddy current losses which generate excessive heat in the windings of transformers and rotating machines leading to acute degradation of winding insulation, reduced dynamic torque, operating noise/mechanical vibration, and a consequent reduction in equipment lifetime [7], [8]. In a four-wire system, the existence of harmonics increases the zero-sequence component of current leading to a sharp increase in neutral conductor current [9], [10]. Harmonics can also increase line phase currents causing false operation of sensitive system components such as protective relays [11], [12]. Telecommunication systems are also affected by harmonics as a result of the effect of electromagnetic emissions [13]. Power Factor Correction Capacitors experience an increased dielectric leakage when the system harmonics increase beyond the fundamental frequency. The circulating reactive current may exceed the maximum current tolerance of the capacitors, leading to early dielectric breakdown [14].

Due to the design simplicity, passive filters have recorded widespread use in harmonics elimination. This form of filters is realized with simple passive elements such as inductors and capacitors, and are categorized based on topology (tuned/damped), or on the connection (shunt/series), or on supply type (e.g. 1-phase-2 wire or 3-phase-3/4 wire) depending on the requirement [15] [16]. For example, [17] proposes a three-phase single-tuned passive filter for a predominant 11^{th} harmonic generated by a twelve-pulse converter. [18] also conducted a similar study by designing a single-tune filter for cancellation of 5^{th} harmonic, coming up with a result of 4.77% of the current Total Harmonic Distortion (THD). Single-tuned filters are effective but are limited to a tuned frequency [20], [21], and are more prone to resonance challenges than other passive filters especially when the Q-factor is not properly selected [22]. For this reason, researchers have come up with different algorithms for optimizing the filtering efficiency of single-tuned filters. For instance,

[23] proposes a Water Cycle Algorithm in designing a single-tuned filter for an inverter-based distribution system. An accurate computing

Technique (particle swamp optimization) for an improved single-tuned harmonic filter has been studied by [24]. An improved single tuned known as a C-type filter has been realised by [25] which can minimize damping losses and marginal resonance damping capabilities. In larger applications, such as arc furnaces and grid PVs, multiple-tuned and damped filters are usually preferable for an improved filtering range of harmonic frequencies [26], [27].

Passive filters have gained a overwhelming recognition in both medium and low-voltage applications. However, these filters present some shortcomings and limitations in their performance which include Inability to adjust to the varying system conditions. In addition, large harmonic current can saturate the filter, leading to the resonating condition due to interaction with the system impedance. They are also bulky in size and weighty in mass which can limit their use in many modern applications.

To overcome these shortcomings, two better filtering technologies which include an Active power filter (APF) and Static Synchronous Compensator (STATCOM) are proposed in this project.

APFs are investigated as a solution to the limitations of conventional passive filters. APFs consists of voltage source converter (VSC) equipped with IGBTs (for active fast switching with low power losses) and passive-energy storage devices for optimum compensation characteristics of voltage and current harmonics filtering; voltage imbalance compensation at the utility site and current imbalance compensation at the consumer site. In addition, APFs mitigate reactive power issues, neutral current, frequency and line impedance variation, voltage notch, sudden voltage distortion, and transient problems and provide power factor improvement in medium-power systems[21].

STATCOM is one of the modern evolutions of flexible ac transmission system (FACTS) controllers in power systems. FACTS controllers are capable of controlling the network condition in a very fast manner and this feature of FACTS can be exploited to mitigate harmonics and transient stabilities of a complex power system[22].

At the distribution level, STATCOM is operated as APF with the capability of fulfilling harmonic mitigation, power factor correction, load balancing and neutral current compensation[3].

APFs/STATCOM have the following advantages over Passive Filters:

- Smaller in physical size and weight compared to passive filter sizes due to passive the passive elements – capacitor(s), inductor(s) and resistor(s).
- Unlike passive filters which are not able to adapt to varying system conditions, Active filters are self-controlled and can adapt continuously to changing system conditions. They are therefore an excellent choice for faster dynamic response.
- They do not pose a risk of harmful resonance to the system.
- Their harmonic response may not be limited to specific as in passive filters, they cover wider harmonic frequency mitigation.
- In addition to current harmonic mitigation, their performance can be extended to load balancing, power factor correction and reactive power compensation [4], [5], [26].

2. METHODOLOGY

To eliminate harmonic with these devices, MATLAB/Simulink (using mathematical models) is used. This involves two essential theories such as Synchronous Reference Frame (SRF) and instantaneous reactive power (PQ) for modelling the APF and STATCOM respectively. The output signals are analyzed with a Fast Fourier Transform (FFT) signal processing toolbox. The analytical results are evaluated based on the IEEE519 standard shown in Table 1.

According to the standard, the harmonic distortion limits for a given non-linear load is determined by the system's Short Circuit Ratio (SCR), defined as the ratio of the peak short circuit current to the peak load current at the PCC. This shows that the standard focuses more on individual harmonics rather than the THD. The first step, therefore, is to determine the system's short circuit ratio, SCR which is given by [2];

$$SCR = \frac{I_{SC}}{I_L} \quad (1)$$

I_{sc} is the peak short circuit current at the PCC = 650.1A and I_L, the peak load current = 162.8A for the model in this study. the I_{sc} is usually obtained from the utility. In this study, it is determined by direct measurement at no load condition [3].

Table 1. IEEE519 standard limits for current harmonics (120V – 69kV)

Maximum Harmonic Current Distortion in Percent of I_L						
	Individual Current Harmonic order, h (odd harmonics)					
SCR (I_{SC}/I_L)	**h<11**	**11≤h <17**	**17≤h<23**	**23≤h <35**	**35≤ h**	**(TDD)**
<20	4.00	2.00	1.50	0.60	0.30	5.0
20<50	7.00	3.50	2.50	1.00	0.50	8.0
50<100	10.00	4.50	4.00	1.50	0.70	12.0
100<1000	12.00	5.50	5.00	2.00	1.00	15.0
>1000	15.00	7.00	6.00	2.50	1.40	20.0
For the even harmonics, the limit is 25% of the odd harmonics presented above SCR: Short circuit ratio TDD: Total demand distortion Isc: Maximum short-circuit current at the point of common connection (PCC) I_L: Maximum demand load current at the point of common connection (PCC)						

$$\therefore\ SCR = \frac{650.1}{162.8} = 3.99$$

This calculation shows that the load should satisfy the harmonic requirement for the SCR below **50** [3] as shown in the Table 1. To analyze the load harmonic condition, FFT analysis is used to obtain the current harmonic spectrum.

2.1 Design Modeling of the APF

Figure 1 shows the APF schematic diagram in a three phase three wire configuration injecting compensating current into the system at the PCC [28], [29], [30].

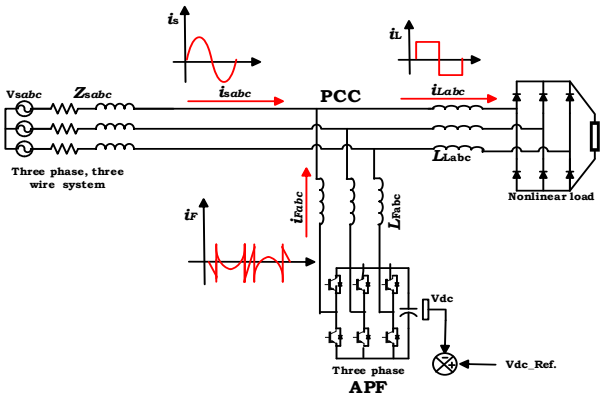

Figure 1. Schematic diagram of Shunt Active Power Filter (SAPF) [28]

APF is basically a voltage source converter (VSC) driven by a separate control system for generating and injecting compensating currents into the system through the following three major tasks: Generation of Reference, tracking of the reference currents and control of the DC-link voltage of the VSC.

2.1.1 Generation of Reference Currents

- Transformations of the three-phase source voltages, and load currents V_{Sabc} and i_{Lab} using Clark's and Park's transformation theories which convert three-phase quantities to two reference frames [31].
- Extraction of harmonic contents using a low pass filter (LPF).
- Taking the inverse of the transformations to obtain equivalent three-phase reference currents.

This process and the rest of the filter control stages are illustrated in the block diagram of Figure 2 [31].

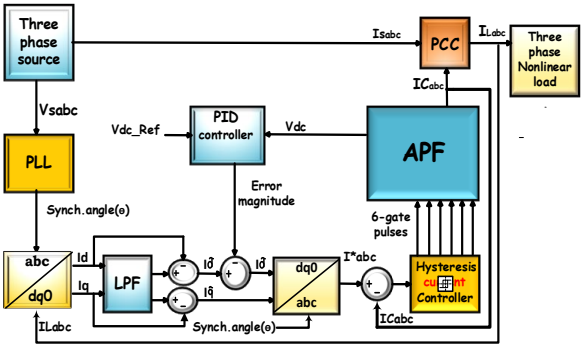

Figure 2. Block diagram of operation and control algorithm of the SAPF for current harmonic elimination.

2.1.1.1 Transformation blocks (synchronous Reference Frame Theory)

To compensate the harmonic contents in the load signals, i_{Labc}, the oscillating components of the currents are required. This is possible with Clark's and Park's transformations which simplifies the stationary three-phase (*abc*) system into two-phase orthogonal system and then into a rotating reference frame termed *dq* (*direct-quadrature*), illustrated in Figure 3 (b).

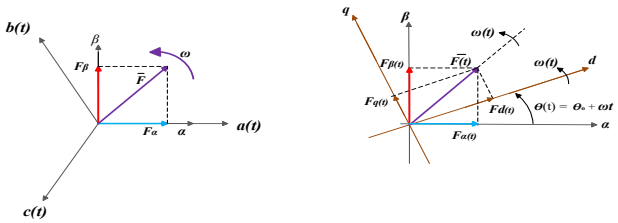

(a) αβ0 reference frame (b) dq0 refence frame

Figure 3. Geometric Representation of Clark's and Park's Transformation [31]

Equations 2 to 4 illustrate the transformation matrix of this geometry for a unit vector, F [31].

$$\begin{bmatrix} F_0 \\ F_\alpha \\ F_\beta \end{bmatrix} = \sqrt{\frac{2}{3}} \begin{bmatrix} \frac{1}{\sqrt{2}} & \frac{1}{\sqrt{2}} & \frac{1}{\sqrt{2}} \\ 1 & \frac{-1}{\sqrt{2}} & \frac{-1}{\sqrt{2}} \\ 0 & \frac{\sqrt{3}}{2} & \frac{\sqrt{3}}{2} \end{bmatrix} \begin{bmatrix} F_a \\ F_b \\ F_c \end{bmatrix} \quad (2)$$

$$\begin{bmatrix} F_d \\ F_q \\ F_0 \end{bmatrix} = \begin{bmatrix} \cos(\omega t) & \sin(\omega t) & 0 \\ -\sin(\omega t) 1 & \cos(\omega t) & 0 \\ 0 & 0 & 1 \end{bmatrix} \begin{bmatrix} F_\alpha \\ F_\beta \\ F_0 \end{bmatrix} \quad (3)$$

$$F_{dq0} = \frac{2}{3} \begin{bmatrix} \cos\theta & \cos(\theta - \frac{2\pi}{3}) & \cos(\theta + \frac{2\pi}{3}) \\ \sin\theta & \sin(\theta - \frac{2\pi}{3}) & \sin(\theta + \frac{2\pi}{3}) \\ \frac{1}{2} & \frac{1}{2} & \frac{1}{2} \end{bmatrix} F_{abc} \quad (4)$$

2.1.1.2 Extraction of the Oscillating Component of Load Current (LPF block)

To separate the two components in each case (oscillating and DC), high order low pass filters (LPF) with a band pass frequency of 20πrad/s is used. With this filter, the DC component are extracted and subtracted from the net frequency, leaving only the oscillating component.

2.1.1.3 Inverse Clark Transformation Block

This block takes the inverse of the dq components (equation 4) of the oscillating currents to obtain the equivalent three phase reference currents i^*_{abc}. Expressed in equations 5 below [31]:

$$i_a^* = i_d sin\theta + i_q cos\theta$$
$$i_{b=}^* i_d \sin\left(\theta - \frac{2\pi}{3}\right) i_q \cos\left(-\frac{2\pi}{3}\right) \quad (5)$$

$$i_c^* \; i_d \sin(\theta \frac{2\pi}{3}) + i_q \cos(\theta + \frac{2\pi}{3})$$

2.2 Tracking of the DC bus Voltage using PID controller (to control switching losses)

For accurate harmonic compensation current, the DC bus voltage has to be kept around a fixed value. However, the APF operation involves high switching frequency. The alternate switching of the inverter results in power loss. In addition, the interfacing reactor also causes power loss. The DC link voltage is therefore installed to ensure power is maintained across the switches. However, this DC bus voltage may collapse after a few seconds because it is a capacitor-sourced voltage.

To keep the DC voltage constant, a control algorithm using a Proportional Integral Differential controller (PID) is employed. this controller ensures Vdc error is minimal by keeping the Vdc as much as possible equal to the reference Vdc. When Vdc falls because of supplying internal power losses, the inverter takes some portion of source currents and converts them into DC for charging the capacitor back to its reference value.

The internal switching losses in the VSC and the losses due to coupling reactance are mainly due to the active component of oscillating current and this is the cumulative steady state error sensed by the PID controller. This mean error (which is actually negative) is added to the oscillating component of I_d to determine the total reference current.

2.3 Tracking of the Reference Currents Using Hysteresis Control Technique

To generate the required firing signals for the APF inverter, the inverter will be operated in such a manner that it will follow the reference currents. To do this, the reference currents, i^*_{abc} are compared with the actual inverter currents, i_{Cabc} and the resulting three-phase error signals are controlled within an envelope or bandwidth along this error signal. This is achieved using hysteresis current control technique. In this technique, the inverter is controlled so that the average variation of the current is nearly sinusoidal by limiting the ripple contents within a hysteresis band. The diagram of Figure 4 shows a πrad sinusoidal reference current (of phase ***a***) within upper and lower band limits.

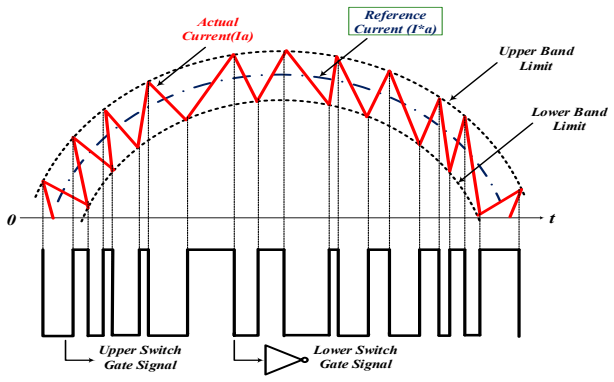

Figure 4. Hysteresis current control technique [31]

2.4 Design Modeling of the STATCOM

The STATCOM is a solid-state device capable of improving the network stability through effective control of reactive power flow within the network. It is one of the modern technologies of Flexible AC Transmission Systems devices popularly known as FACTS [3]. Like APF, which is basically a VSC, STATCOM has additional features of synchronous motor. It becomes capacitive when overexcited and inductive when under excited by varying the voltage angle through built-in DC bus voltage [3]. STATCOM injects reactive power to the grid when its voltage rises above the grid voltage and absorbs same when the reverse is the case. When grid and the STATCOM have equal voltages, there will be no interaction between the two, hence the power factor (PF) ideally becomes unity [4]. For elimination of harmonics, the schematic is in the same way as is APF as shown in Figure 5.

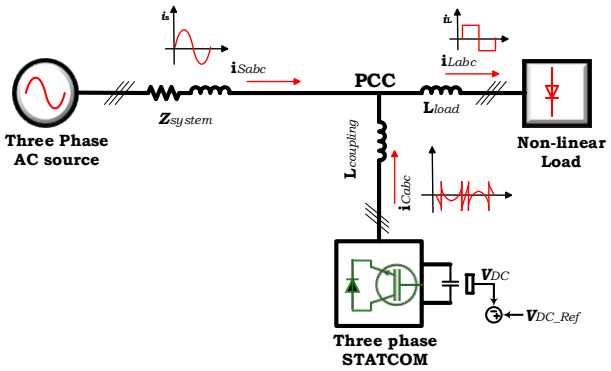

Figure 5. Schematic diagram of a STATCOM connected at the system's PCC [4]

The device operation is largely dependent on the control system which is achieved with Instantaneous Reactive Power (IRP or PQ) theory through the following operational sequence:

2.4.1 Generation of Reference Current

The first stage in the modeling using PQ [4] (or pq) theory is the generation of reference current as follows:

- Transformation of the three-phase source voltages and load currents into two-phase, αβ0 known as Clark's Transformation.
- Establishing instantaneous active and reactive power from the transformed quantities (αβ0).
- Identification and extraction of oscillating components of the established powers using low pass filters (LPF).
- In terms of the oscillating values of power, αβ0 components of current are generated. The inverse transformation of this αβ0 gives the three phase reference currents *I*abc.*

The block diagram of Figure 6 gives a clear illustration of the whole processes involved, from transformation (first stage) to compensation current stage (last stage).

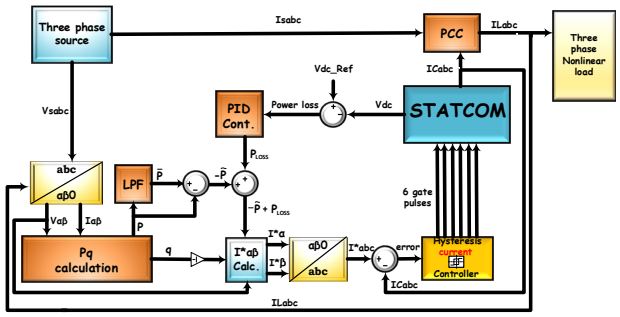

Figure 6. Block diagram of a STATCOM using *pq* control technique [4]

2.4.1.1 Clark's Transformation (abc to αβ0 block)

As shown in Figure 6 the source voltages, V_{abc}, and the load currents, I_{abc}, are measured and transformed into αβ0 using Clark's transformation [4] (*abc to αβ0 reference frame*) illustrated in the geometry of Figure 7.

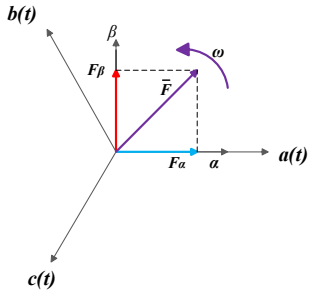

Figure 7. geometric representation of Clark's Transformation [4]

From this geometry, the following resolutions can be generated in terms of α and β frames [10]:

$$\begin{bmatrix} V_0 \\ V_\alpha \\ V_\beta \end{bmatrix} = \sqrt{\frac{2}{3}} \begin{bmatrix} \frac{1}{\sqrt{2}} & \frac{1}{\sqrt{2}} & \frac{1}{\sqrt{2}} \\ 1 & \frac{-1}{\sqrt{2}} & \frac{-1}{\sqrt{2}} \\ 0 & \frac{\sqrt{3}}{2} & \frac{-\sqrt{3}}{2} \end{bmatrix} \begin{bmatrix} V_a \\ V_b \\ V_c \end{bmatrix} \quad (6)$$

$$\begin{bmatrix} i_0 \\ i_\alpha \\ i_\beta \end{bmatrix} = \sqrt{\frac{2}{3}} \begin{bmatrix} \frac{1}{\sqrt{2}} & \frac{1}{\sqrt{2}} & \frac{1}{\sqrt{2}} \\ 1 & \frac{-1}{\sqrt{2}} & \frac{-1}{\sqrt{2}} \\ 0 & \frac{\sqrt{3}}{2} & \frac{-\sqrt{3}}{2} \end{bmatrix} \begin{bmatrix} i_a \\ i_b \\ i_c \end{bmatrix} \quad (7)$$

2.4.1.2 Calculation of instantaneous Active and Reactive Powers (pq) block

For a balanced three phase supply, the zero sequence components V_0 and I_0 become 0. In this case, the instantaneous real and reactive power (p and q) can be obtained from the instantaneous phase voltages and load currents on the αβ0 axis as [4];

$$p = v_\alpha i_\alpha + v_\beta i_\beta$$

$$q = -v_\beta i_\alpha + v_\alpha i_\beta \quad (8)$$

$$p = v_0 i_0 = 0$$

The reactive power, q is just a fictitious value. The matrix representation of the equations is given by [4];

$$\begin{bmatrix} p \\ q \end{bmatrix} = \begin{bmatrix} v_\alpha & v_\beta \\ -v_\beta & v_\alpha \end{bmatrix} \begin{bmatrix} i_\alpha \\ i_\beta \end{bmatrix} \quad (9)$$

2.4.1.3 Extraction of the Oscillating Components of p & q (LPF block)

For the fact that i_α and i_β are non-sinusoidal (due to harmonics), both *p* and *q* are equally non-sinusoidal. When the voltage and currents are sinusoidal and in phase, the reactive component *q* will not exist and the active component, *p* will have some *DC* value. However, due to the presence of harmonics, equations 10 and 11 represent the actual power in the system [10].

$$P = p_{ac} + P_{dc} \quad (10)$$

$$q = q_{ac} + q_{dc} \quad (11)$$

Now to eliminate harmonics, $-p_{ac}$ and $-q$ will be injected into the grid to nullify the existing p_{ac} and q components. The magnitude of $-p_{ac}$ is manipulated with the use of LPF and the magnitude of '$-q$' is determined by direct inversion of the q component as shown in the block diagram. These are the respective active and reactive powers required for the generation of reference currents. Therefore, from equation 9, we have [10];

$$\begin{bmatrix} i_\alpha^* \\ i_\beta^* \end{bmatrix} = \frac{1}{v_\alpha^2 + v_\beta^2} \begin{bmatrix} v_\alpha & -v_\beta \\ v_\beta & v_\alpha \end{bmatrix} \begin{bmatrix} p \\ q \end{bmatrix} \quad (12)$$

Substituting p and q with $-p_{ac}$ and $-q$ yields equation 13[10].

$$\begin{bmatrix} i_\alpha^* \\ i_\beta^* \end{bmatrix} = \frac{1}{v_\alpha^2 + v_\beta^2} \begin{bmatrix} v_\alpha & -v_\beta \\ v_\beta & v_\alpha \end{bmatrix} \begin{bmatrix} -p_{ac} + p_{Loss} \\ -q \end{bmatrix} \quad (13)$$

p_{Loss} is a small amount of average real power drawn by the STATCOM to maintain a constant DC-bus voltage which is explained in the next topic.

2.4.1.4 Tracking the DC-bus voltage using PID controller

As was the case of APF, the continuous energy loss due high converter switching frequency can result in a gradual discharge of the supplying capacitors and will eventually become zero. In this case also, an external PID controller is employed to keep the capacitor voltage at a set value of 563 V which is sufficient enough to sustain the loss occurring within the device VSC. As shown in the block diagram of Figure 6, the difference between the set value and the DC-bus voltage (p_{Loss}) is fed to the PID controller for compensation of the loss. Therefore, in addition to the compensating component of active power ($-p_{ac}$), the STATCOM must also draw this amount of power loss as shown in equation 13.

The three phase components of reference current (i^*_{abc}) can be deduced by simply taking the inverse Clark's transformation of equation 14 yielding the following relation [10];

$$\begin{bmatrix} i_a^* \\ i_b^* \\ i_c^* \end{bmatrix} = \sqrt{\frac{2}{3}} \begin{bmatrix} 1 & 0 \\ \frac{-1}{2} & \frac{\sqrt{3}}{2} \\ \frac{-1}{2} & \frac{\sqrt{3}}{2} \end{bmatrix} \begin{bmatrix} i_\alpha \\ i_\beta \end{bmatrix} \quad (14)$$

Finally, the generated reference current is controlled using hysteresis control technique explained in APF section, for the generation of firing signals to the gates of the inverter switches with a ripple-free compensation current waveform.

2.5 Simulation of the Design Using MATLAB / SIMULINK Software

Based on the foregoing mathematical models and the design parameters summarized in Table 2, the harmonic mitigation performance of the two devices is validated using MATLAB/Simulink.

Table 2. Simulation design parameters [4]

Parameter	Description
Supply	3-Ø, 500 kVA, 11 kV/400 V transformer fed from 11 kV, 50 Hz source with line impedance of 1 Ω, 1 mH
Load	38.8kW (RL load; DC Motor; Battery Charging system)
APF & STATCOM converter rating	40 kVA (minimum requirement)
Inverter DC bus voltage	653 V
Inverter DC bus capacitor	6000 µF
Coupling inductor	1.2m H
Kp, Ki (APF)	0.5, 50
Kp, Ki (STATCOM)	1, 25

The simulation models for the APF and STATCOM are respectively shown in Figures 8 and Figure 9. Each of the models comprises three main subsystems – the supply, the load, and the Mitigation device with its control system. The PCC is the bus where the devices are connected. Other consumers within the network are also connected at this point.

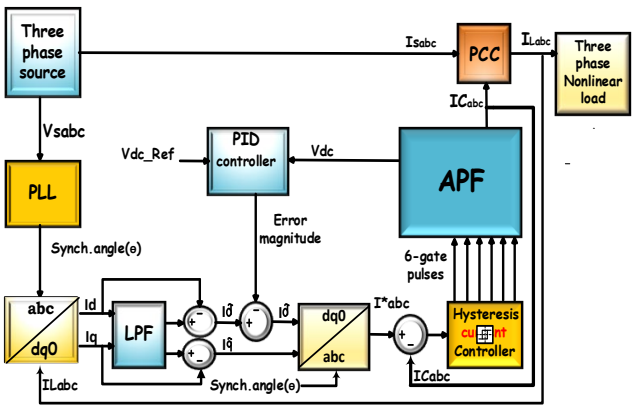

Figure 8. MATLAB Simulation Model for AFP [4]

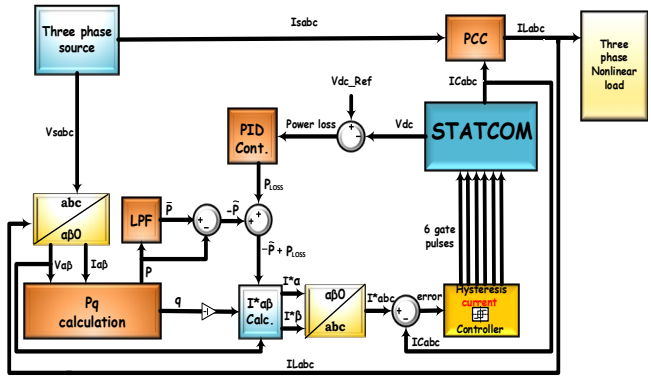

Figure 9. MATLAB Simulation Model for STATCOM [4]

3. RESULTS AND DISCUSSION

The system's load signals before and after APF action are illustrated in Figure 10. Figures 11 and Figure 12 show the FFT analysis of the percentage harmonic distortions before and after mitigation using the APF. The APF can successfully eliminate the harmonic in the signal by THD level of 14.52%. Similarly, Figures 13, Figure 14 and Figure 15 illustrate the same conditions when STATCOM is used instead. These proves that STATCOM is better than APF in eliminating harmonic since the THD level is lower compared to when APF is used. The THD level is only 0.24% where STATCOM can be used for harmonic elimination. STATCOM is a kind of FACTS devices that can be used for harmonic distortion since it can eliminate all the unwanted signal in the waveform.

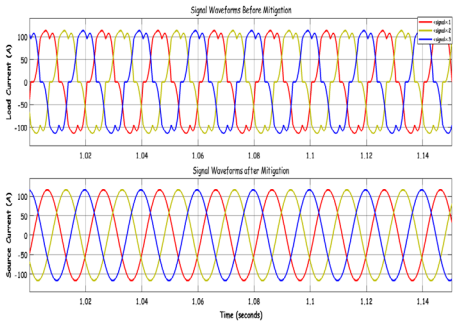

Figure 10. The load waveforms before and after mitigation using APF

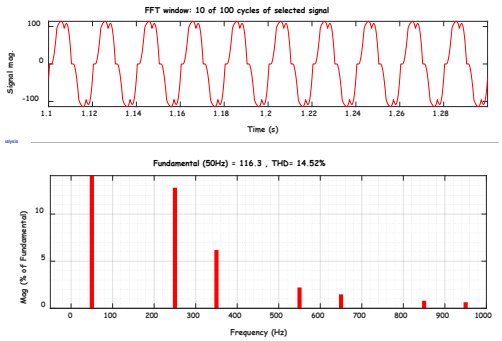

Figure 11. FFT analysis of the % distortion before mitigation using APF

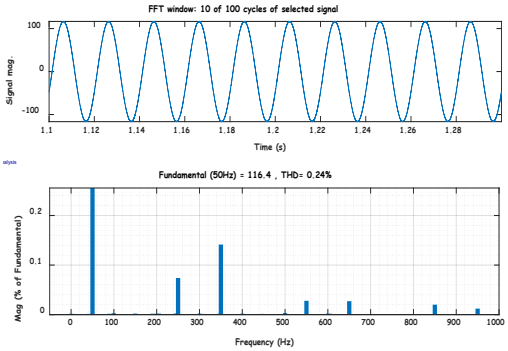

Figure 12. FFT analysis of the % distortion after mitigation using APF

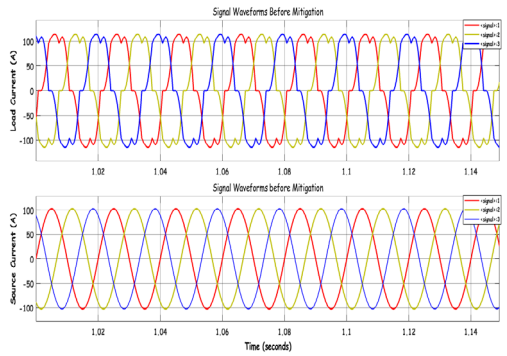

Figure 13. The load waveforms before and after mitigation using STATCOM

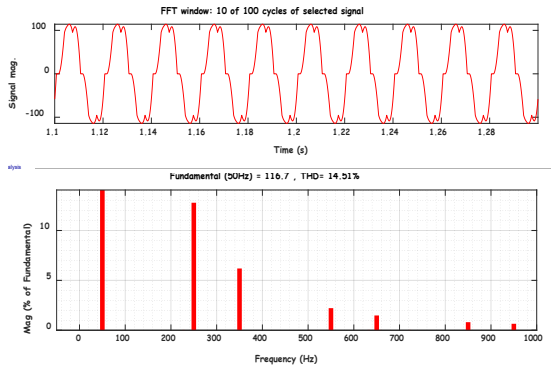

Figure 14. FFT analysis of the % distortion before mitigation using STATCOM

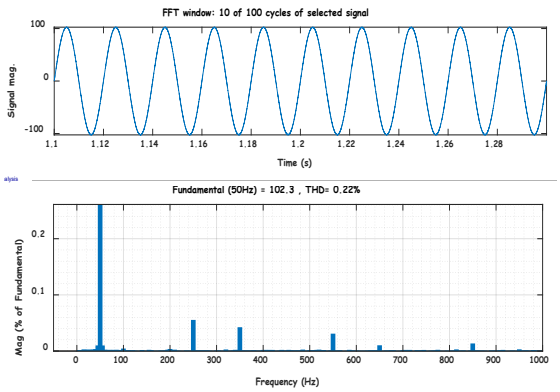

Figure 15. FFT analysis of the % distortion after mitigation using STATCOM

3.1 The Simulink FFT Analysis and Performance Evaluation Results of the two Devices

From the fast Fourier transform (FFT) analyses of Figure 11, Figure 12, Figure 14 and Figure 15, the percentage distortion for the individual odd harmonics from 7th to 19th has been generated for each. These are presented in Table 3.

Table 3. The system harmonic conditions before and after mitigation

	APF		STATCOM		
	Before (%)	**After (%)**	**Before (%)**	**After (%)**	**IEEE519 Standard (%)**
TDD	14.52 *	0.24	14.52 *	0.22	5.0
h_5	12.78 *	0.77	12.78 *	0.55	4.0
h_7	6.18 *	0.14	6.18 *	0.042	4.0
h_{11}	2.22 *	0.03	2.22 *	0.031	2.5
h_{13}	1.48	0.03	1.48	0.01	2.5
h_{17}	0.81	0.02	0.81	0.014	1.5
h_{19}	0.65	0.01	0.65	0.00	1.5

Table 3 presents the results of the system harmonic condition and the respective performance of the two devices before and after mitigation. Column 1 contains the total demand distortion (TDD) as well as the individual odd harmonics existing in the system between 5th and 19th order. The harmonics frequencies with the multiple of 3 such as 3rd, 9th and 15th do not exist in the system because they are in zero sequence which can only be considered in a three phase, four wire system.

Column 2 and 4 show the system's harmonic conditions when neither of the devices is put into action. Those condition extending beyond the IEEE519 limits (column 6) are indicated by the red asterisks. It can be noted that the total demand distortion (TDD) is 14.52%, close to two times the standard limit of 8%. With APF, this magnitude has been suppressed to 0.24% and with the STATCOM, the value is adjusted it to 0.22% as shown, respectively, in columns 3 and 5. In both cases, the current harmonics have been sufficiently minimized.

Similarly, 5th order harmonics, the most prevalent in the model, has been clipped from 12.78% to 0.77 and 0.55 by the APF and STATCOM respectively. The 7th and 11th order harmonics which are also beyond the standard have been suppressed to the lowest fractions as shown in the table.

4.0 CONCLUSION AND RECOMMENDATION

The design and simulation of the APF and STATCOM has been successfully implemented and their performances in mitigating current harmonics (in consonant with the IEEE519 standard) has also been satisfactorily achieved. Passive filters can also do the same task but with limitations to certain harmonic frequencies which is not desirable in a system with varying loads. With these devices however, the suppression of all higher order harmonics is made possible. Based on the performance evaluation from the simulation results, the STATCOM presents a better performance profile for harmonic mitigation as compared to APF. In practical situations, the supply may also be distorted due to voltage umbalance. It is, therefore, recommended for further study, the design of

a sensing circuit to be incorporated that will maintain the positive sequence of the fundamental voltage. For this paper, it is assumed positive.

REFERENCES

[1] M. E. Farrag, A. Haggag, H. Farooq, and W. Ali, "Analysis and mitigation of harmonics caused by air conditioners in a distribution system," *2017 19th Int. Middle-East Power Syst. Conf. MEPCON 2017 - Proc.*, vol. 2018-Febru, no. December, pp. 702–707, 2018, doi: 10.1109/MEPCON.2017.8301258.

[2] A. Abd El-Mageed Elhenawy, M. Mohamed Sayed, and M. Ibrahim Gilany, "Harmonic Cancellation in Residential Buildings," *2018 20th Int. Middle East Power Syst. Conf. MEPCON 2018 - Proc.*, no. 1, pp. 346–351, 2019, doi: 10.1109/MEPCON.2018.8635171.

[3] P. Chiradeja, A. Ngaopitakkul, and C. Jettanasen, "Energy savings analysis and harmonics reduction for the electronic ballast of T5 fluorescent lamp in a building's lighting system," *Energy Build.*, vol. 97, pp. 107–117, 2015, doi: 10.1016/j.enbuild.2015.03.042.

[4] W. Ahmed, N. Ali, M. S. Nazir, and A. Khan, "Power quality improving based harmonical studies of a single-phase step-down bridge-cycloconverter," *J. Electr. Syst.*, vol. 15, no. 1, pp. 109–122, 2019.

[6] E. Cuce, P. Mert, F. Gul, and A. Iskendero, "Harmonic problems in renewable and sustainable energy systems: A comprehensive review," vol. 48, no. September, 2021, doi: 10.1016/j.seta.2021.101566.

[7] M. A. Taher, S. Kamel, and Z. M. Ali, "K-Factor and transformer losses calculations under harmonics," *2016 18th Int. Middle-East Power Syst. Conf. MEPCON 2016 - Proc.*, pp. 753–758, 2017, doi: 10.1109/MEPCON.2016.7836978.

[8] J. Hernández, A. A. Romero, J. Meyer, and A. M. Blanco, "Impact of nonlinear lighting loads on the neutral conductor current of low voltage residential grids," *Energies*, vol. 13, no. 18, 2020, doi: 10.3390/en13184851.

[10] J. Sutaria, A. Espin-Delgado, and S. Ronnberg, "Summation of Supraharmonics in Neutral for Three-Phase Four-Wire System," *IEEE Open J. Ind. Appl.*, vol. 1, no. October, pp. 148–156, 2020, doi: 10.1109/ojia.2020.3026753.

[11] A. Benjamin and S. K. Jain, "A Review of Literature on Effects of Harmonics on Protective Relays," *Int. Conf. Innov. Smart Grid Technol. ISGT Asia 2018*, pp. 407–412, 2018, doi: 10.1109/ISGT-Asia.2018.8467876.

[12] K. Wannous and P. Toman, "Evaluation of harmonics impact on digital relays," *Energies*, vol. 11, no. 4, 2018, doi: 10.3390/en11040893.

[13] M. Z. Mohd Radzi, M. M. Azizan, and B. Ismail, "Observatory case study on total harmonic distortion in current at laboratory and office building," *J. Phys. Conf. Ser.*, vol. 1432, no. 1, 2020, doi: 10.1088/1742-6596/1432/1/012008.

[14] M. M. Islam, D. Sutanto, and K. M. Muttaqi, "Protecting PFC capacitors from overvoltage caused by harmonics and system resonance using high temperature superconducting reactors," *IEEE Trans. Appl. Supercond.*, vol. 29, no. 2, 2019, doi: 10.1109/TASC.2019.2895269.

[15] M. S. Almutairi and S. Hadjiloucas, "Harmonics mitigation based on the minimization of non-linearity current in a power system," *Designs*, vol. 3, no. 2, pp. 1–16, 2019, doi: 10.3390/designs3020029.

[16] A. Baitha and N. Gupta, "A comparative analysis of passive filters for power quality improvement," *Proc. IEEE Int. Conf. Technol. Adv. Power Energy, TAP Energy 2015*, pp. 327–332, 2015, doi: 10.1109/TAPENERGY.2015.7229640.

[17] T. M. Aye and S. W. Naing, "Analysis of Harmonic Reduction by using Passive Harmonic Filters," *Int. J. Sci. Eng. Technol. Res.*, vol. 03, no. 45, pp. 9142–9147, 2014, [Online]. Available: www.ijsetr.com

[18] S. S. Saha and R. Suryavanshi, "Power system harmonic mitigation of an offshore oil rig using passive shunt filter," *Proc. 2010 Annu. IEEE India Conf. Green Energy, Comput. Commun. INDICON 2010*, pp. 5–9, 2010, doi: 10.1109/INDCON.2010.5712729.

[19] M. Bradt *et al.*, "Harmonics and resonance issues in wind power plants," *Proc. IEEE Power Eng. Soc. Transm. Distrib. Conf.*, pp. 1–8, 2012, doi: 10.1109/TDC.2012.6281633.

[20] C. Boonseng, N. Nilnimitr, and K. Kularbphettong, "An Investigation on the Selection of Filter Topologies for Passive Filter Applications by Neural Network," *Proc. 2019 Int. Conf. Power, Energy Innov. ICPEI 2019*, vol. 24, no. 3, pp. 48–51, 2019, doi: 10.1109/ICPEI47862.2019.8944934.

[21] Y.-S. Cho and H. Cha, "Single-tuned Passive Harmonic Filter Design Considering Variances of Tuning and Quality Factor," *J. Int. Counc. Electr. Eng.*, vol. 1, no. 1, pp. 7–13, 2011, doi: 10.5370/jicee.2011.1.1.007.

[23] M. Dzar Faraby, A. Fitriati, Christiono, Usman, A. Muchtar, and A. Nur Putri, "Single Tuned Filter Planning to Mitigate Harmonic Polluted in Radial Distribution Network Using Particle Swarm Optimization," *2020 3rd Int. Semin. Res. Inf. Technol. Intell. Syst. ISRITI 2020*, no. 1, pp. 418–422, 2020, doi: 10.1109/ISRITI51436.2020.9315518.

[25] S. H. E. Abdel Aleem and A. F. Zobaa, "Optimal C-type filter for harmonics mitigation and resonance damping in industrial distribution systems," *Electr. Eng.*, vol. 99, no. 1, pp. 107–118, 2017, doi: 10.1007/s00202-016-0406-1.

[26] R. N. Beres *et al.*, "Optimal Design of High-Order Passive-Damped Filters for Grid-Connected Applications," vol. 8993, no. c, 2015, doi: 10.1109/TPEL.2015.2441299.

[27] H. Singh, M. Kour, D. V. Thanki, and P. Kumar, "A review on Shunt active power filter control strategies," *Int. J. Eng. Technol.*, vol. 7, no. 4, pp. 121–125, 2018, doi: 10.14419/ijet.v7i4.5.20026.

[29] S. Agrawal, D. K. Palwalia, and M. Kumar, "Performance Analysis of ANN Based three-phase four-wire Shunt Active Power Filter for Harmonic Mitigation under Distorted Supply Voltage Conditions," *IETE J. Res.*, vol. 68, no. 1, pp. 566–574, 2022, doi: 10.1080/03772063.2019.1617198.

[30] E. Sundaram and M. Venugopal, "On design and implementation of three phase three level shunt active power filter for harmonic reduction using synchronous reference frame theory," *Int. J. Electr. Power Energy Syst.*, vol. 81, pp. 40–47, 2016, doi: 10.1016/j.ijepes.2016.02.008.

[32] L. Dinesh, H. Sesham, and V. Manoj, "Simulation of D-Statcom with hysteresis current controller for harmonic reduction," *Proc. - ICETEEEM 2012, Int. Conf. Emerg. Trends Electr. Eng. Energy Manag.*, pp. 104–108, 2012, doi: 10.1109/ICETEEEM.2012.6494513.